Chapter 2
Use of Carbon Nanotubes in Photoactuating Composites

2.1 Introduction

The direct conversion of light energy into to mechanical motion, the optomechanical effect, is also termed photostriction or photoactuation. Photostrictive materials are scarce but the technology is of significant interest with applications ranging from civil infrastructures to medicine to the aerospace industry to telecommunications. These types of smart materials are expected to be able to produce a variety of devices and are envisioned to be used as light-driven motors, for energy scavenging, artificial muscles, and tactile displays. The development goals for photoactuators include large range of motion, high precision, high speed, high strain energy density, and low fatigue rate. Ideally, these types of materials could be used in both microelectromechanical and nanoelectromechanical systems.

Carbon nanotubes (CNTs) have been use to construct electrically driven actuators using a variety of structures [1–7]. Generally, in the electrically driven systems the charge separation at or near the electrodes effect the biggest component of the volume change. There has been a flurry of theoretical activity to understand the mechanical properties of CNTs [8–19]. However, none of these reports considered the effect of light on the stress/strain behavior of CNTs.

CNTs can be observed to photoactuate under a variety of motifs, including freestanding bundles [20, 21], pure CNT films [22], mixed into polymer hosts [23–27], and as part of layered composites [28–33]. While the magnitude of the volume response under exposure to light is remarkably large in all cases, the exact composition and preparation method used to make the photoactuator appears to have an influence on the underlying mechanism.

I. A. Levitsky et al., *Photophysics of Carbon Nanotubes Interfaced with Organic and Inorganic Materials*, DOI: 10.1007/978-1-4471-4826-5_2,

2.2 Carbon Nanotube Bundles and Freestanding Films

2.2.1 Freestanding Bundles

Zhang and Iijima [20] were the first to report photoactuation in carbon nanotubes in 1999. Laser ablation of a graphite target (impregnated with metal catalysts) gave single-walled carbon nanotubes deposited onto Kovar electrodes. The SWNTs deposited as bundles consisting of filaments with lengths up to 1 mm and diameters of about 10 μm. The filaments extended between the two electrodes and could be affixed to one electrode or to both electrodes, depending upon the experiment.

Using a white light (halogen lamp) with an intensity of about 20 mW/cm^2 the tip displacement of a ~1 mm long, 10 μm diameter filament could be as high as 170 μm with the time frame for full response being on the order of 100 ms. For thicker filaments, 50–100 μm, the bending displacement reached as high as 1.3 mm. The magnitude of the displacement was found to depend upon the intensity of the light in the visible region but not upon the wavelength. This latter conclusion was based upon a comparison between the white light of the halogen source with different color filters and a single laser wavelength, 633 nm from a He–Ne laser. No investigation of using light in the near infrared region was reported.

Figure 2.1 shows the behavior of one of these filaments under several different illumination conditions. Under high intensity illumination, Fig. 2.1a (white light, ~30 mW/cm^2) and c (633 nm light, ~800 mW/cm^2), the tip of the SWNT filament formed a loop, as denoted by the arrows, and the mechanical motion was independent of the color of the light. When the intensity of the light is reduced to ~5 mW/cm^2, Fig. 2.1b (white light), a loop no longer forms. Rather, there is simply bending of the tip of the filament. For comparison purposes, Fig. 2.1d, the same filament was exposed to an electric field in the dark and a loop similar to those found under strong illumination was found.

Zhang and Iijima attributed the photoactuation in the SWNT bundles to an electrostatic effect. They arrived at this conclusion primarily because of the similar mechanical deformation observed under light or an electric field. A photon pressure effect was eliminated since the bending did not always match the orientation of the light source. Thermal expansion was thought to be unlikely because of the large magnitude of the displacements observed. The proposed mechanism was that the light induced a photocurrent in the nanotubes. Since the filaments are composed of nonuniform bundles of SWNTs, a local charge accumulation could result, especially at bends in the filaments. The local charge then creates an electrostatic field that leads to repulsion between different nanotubes within the filament. Depending upon the diameter of the filament and the amount of light absorbed, different directions of bending could be observed.

Cronin et al. [21] measured the Raman spectra of individual SWNTs and were able to deduce certain characteristics of the change in shape of the nanotubes under irradiation. SWNTs were grown suspended across a trench and the Raman spectrum measured with a tunable laser at ~1 mW power. The Stokes/anti-Stokes

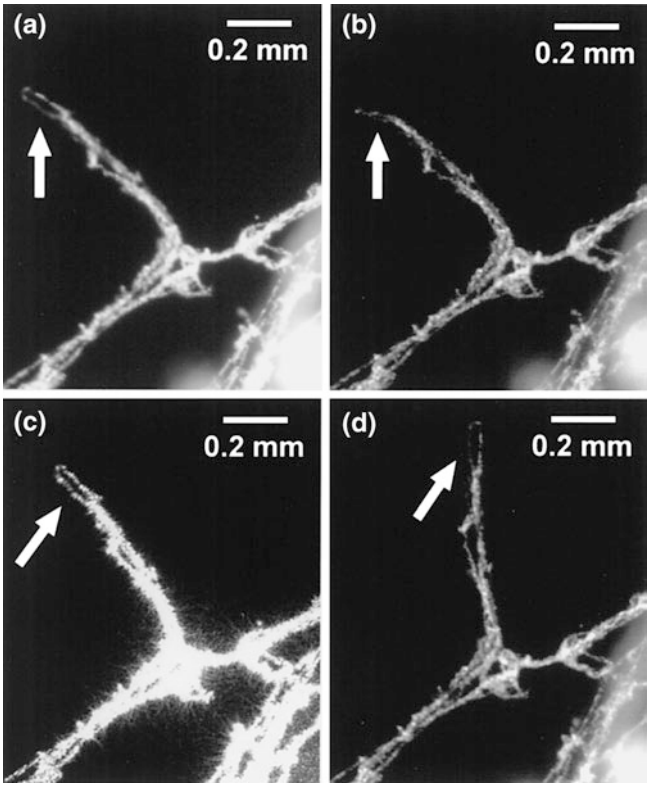

Fig. 2.1 A SWNT filament under different illumination conditions: **a** 30 mW/cm^2 *white* light source (halogen lamp); **b** 5 mW/cm^2 *white* light **c** 800 mW/cm^2 He–Ne laser (633 nm); **d** no illumination but in an electric field. Reprinted Fig. 2.3 with permission from Ref. [20]. Copyright 1999 by the American Physical Society

ratio indicated that the laser caused minimal temperature change in each sample. The results implied a strong electron–phonon coupling and that radial expansion, not axial elongation, was responsible for the observed results. Although no photoactuation was directly observed, the results imply that the radial expansion of the SWNTs can be significant.

2.2.2 Freestanding Films

Ahir et al. [22] prepared free standing films of both MWNTs and SWNTs. The nanotubes were dispersed in isopropyl alcohol, ~0.1 mg/mL, using ultrasonication but no surfactant. The dispersion was vacuum filtered through a filter composed of a mixed cellulose ester. The thickness of the SWNT layer was controlled

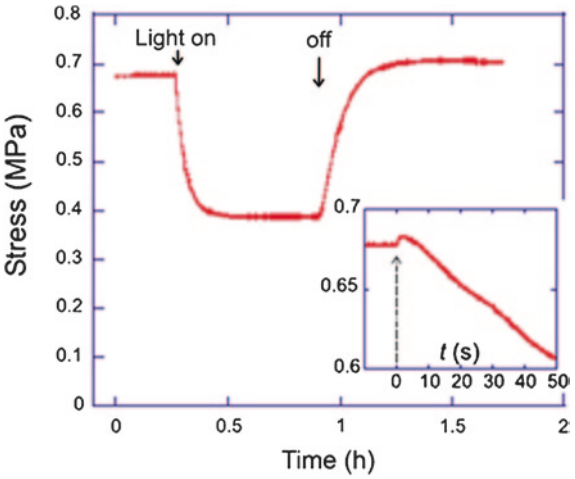

Fig. 2.2 Stress response of a MWNT film under 675 nm light. The *inset* shows an expansion of the first few seconds of the measurement in the light-on regime. Reprinted Fig. 2.6 with permission from Ref. [22]. Copyright 2007 by the American Physical Society

by varying the concentration of the nanotubes in the dispersion. The filter membrane containing the nanotube layer was rinsed and dried and the resulting films could be peeled off of the filter membrane. The photoactuation experiments were done using a LCD light source with maximum output at 675 nm and a breadth ranging from ~500 to ~800 nm. The sample was uniformly illuminated and the incident intensity was ~1.5 mW/cm^2 at 675 nm. The samples were clamped to supports placed into a thermally controlled housing. A dynamometer was used to exert force on the sample and the length of the sample could be measured to 1 μm precision.

The photoactuation of a MWNT film is shown in Fig. 2.2. When the light is turned on the stress drops, indicating that the sample is expanding, i.e., experiencing tension. The time constant for the photoactuation is on the order of 10 s of minutes. When the light is turned off, the sample returns to its original state, exhibiting a fully reversible response. However, at very short times the initial photoactuation is an increase in stress, i.e. compression. This initial event is complete in seconds. The same two directional response is observed when the light is turned off (not shown in the figure): an initial drop in stress for a few seconds and then an increase in stress until the initial state is recovered.

The response of the SWNT film is completely different, as shown in Fig. 2.3. Upon exposure to the light, the SWNT film shows an increase in stress, i.e., compression. The time constant is fast, on the order of seconds. The SWNT films exhibit a slight fade in the stress after reaching the maximum value while the light is on. When the light is turned off, the film rapidly relaxes to its initial state, again with a time constant on the order of seconds. The SWNT films do not show the small initial feature that was observed for the MWNT films. Independent experiments using a standard heating source showed smaller stress changes, indicating that the observed response is not a simple heating effect.

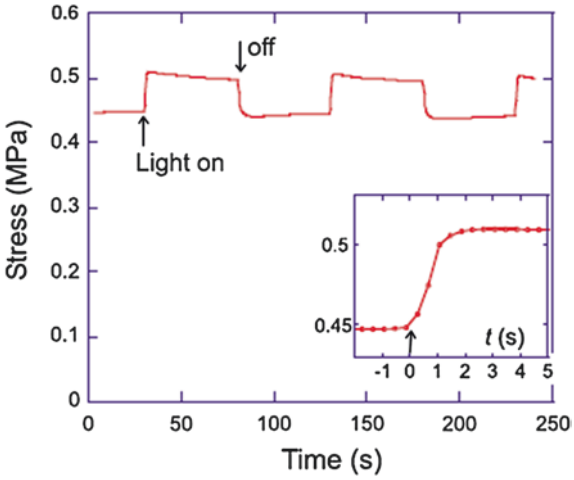

Fig. 2.3 Stress response of a SWNT film under 675 nm light. The *inset* shows an expansion of the first few seconds of the measurement in the light-on regime. Reprinted Fig. 2.7 with permission from Ref. [22]. Copyright 2007 by the American Physical Society

The authors explained the differences between the MWNT and SWMT freestanding films based on the network behavior of each type of nanotube. The MWNT were envisioned as a granular network. In contrast, the SWNT was described to be more like a cross-linked polymer network.

2.3 Carbon Nanotubes in Mixed Composites

2.3.1 Rubbery Polymer Host Materials

In a series of papers, Terentjev et al. [23–26] examined the photoactuation of carbon nanotubes mixed into rubbery polymers. Most of their research was done using poly (dimethylsiloxane) (PDMS) but they also reported studies in poly (styrene–isoprene-styrene) triblock polymer (SIS), and monodomain and polydomain liquid crystal elastomers. The nanotubes were multiwalled and were thoroughly mixed into the rubber host prior to polymerization. Great care was taken to insure that the MWNTs were completely dispersed in the host system. Loadings of the MWNTs ranged from 0 to 7 wt%. Samples loaded with 3 wt% carbon black were also prepared for comparison. Fibers were drawn from the cured polymer and samples were cut into cantilevers of dimensions 30 mm long $\times$ 1.5 mm wide $\times$ 0.2 mm thick. Samples were pre-stretched to a determined amount of strain prior to measuring the photoactuation, with pre-strain values ranging from 2 to 40 % ($\varepsilon = 0.02 - 0.40$).

The photoactuation experiments were done using a LCD light source with maximum output at 675 nm and a breadth ranging from ~500 to ~800 nm. The sample was uniformly illuminated and the incident intensity was ~1.5 mW/cm^2 at 675 nm.

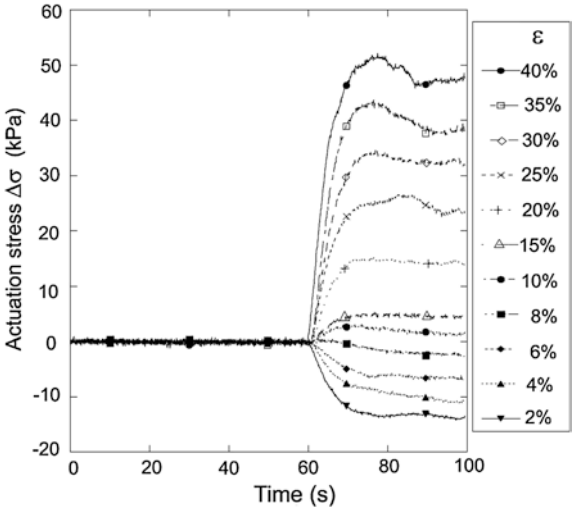

Fig. 2.4 Stress response of a PDMS sample containing 3 wt% MWNTs. The different curves show the photoactuation with different pre-strain levels. The light is turned on at t = 60 s. Reprinted Fig. 2.8 with permission from Ref. [25]. Copyright 2006 by the American Physical Society

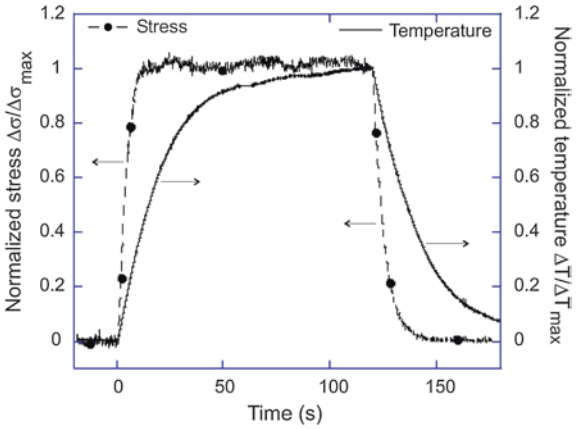

Fig. 2.5 A comparison of the normalized stress response (*dashed line*, *left axis*) and the normalized temperature response (*solid line*, *right axis*) for a PDMS sample containing 3 wt% MWNTs and a pre-strain of 20 % upon exposure to light. Reprinted Fig. 2.9 with permission from Ref. [25]. Copyright 2006 by the American Physical Society

The samples were clamped to supports placed into a thermally controlled housing. A dynamometer was used to exert force on the sample and the length of the sample could be measured to 1 μm precision. Absorption measurements of the host material showed that ~30 % of the incident light was absorbed or scattered but even low loadings of MWNTs (0.3 wt%) caused more than 97 % of the light to be absorbed. The spectrum of the MWNTs in the host polymers was featureless, only displaying a slight rise from 1000 to 300 nm. The composites were pre-strained in the apparatus to a determined value, allowed to relax for 10 min, and then stress measurements were taken. Thermocouples were placed on both sides of the sample to determine the temperature change across the sample during illumination.

Figure 2.4 shows the results of the measured stress of a PDMS sample as a function of time when the light is turned on. There is a strong dependence of the

photoresponse on the amount of pre-strain induced in the sample. At low pre-strain the stress a negative stress is measured, indicative of tension in the sample. At higher pre-strains the stress reverses to a positive value, meaning that the sample experiences compression during photoactuation. This type of behavior was observed for all hosts and the crossover point from tension to compression was found to be for pre-strains of 6–10 %. The time to reach maximum strain is 10–15 s for all samples. The time dependence was fit to a compressed exponential of the form $1 - \exp(-(t/\tau)^{\beta})$ where the time constant, τ, is ~5 s and the exponent, β, is ~2 were constant at sufficiently high loadings of MWNTs. The response was slower when the concentration of MWNTs was below the percolation threshold with τ ~10 s and β ~1. The decay of the photoinduced stress (not shown) follows a simple exponential function, $\exp(-t/\tau)$, with the relaxation time, τ, ~5 s.

To understand the relationship between the photoactuation and the temperature change, a direct measurement of the temperature change across the sample was made during exposure to light. While the temperature change depended upon the loading of the MWNTs, typical values were ΔT ~15 °C. A plot of the normalized temperature change and the normalized stress change as a function of exposure time is shown in Fig. 2.5. The difference in the response of the two measurements is striking. As discussed above, upon light exposure the stress reaches is maximum value in 10–15 s. In contrast, the thermal response is ~10× slower, taking 100–150 s to reach the equilibrium temperature. This indicates that the stress response is not primarily caused by simple heating effects. To confirm this, the authors measured the stress when samples were raised to the same temperature by a mica-insulated heater. Under these conditions the stress response was 10 times smaller than when exposed to light.

Figure 2.6 shows the change in stress as a function of loading and applied pre-strain for PDMS as the host. Remarkably, the transition from tension to compression is essentially constant for all MWNT loadings. Figure 2.6 also shows the strain calculated using the observed stress and Young's modulus.

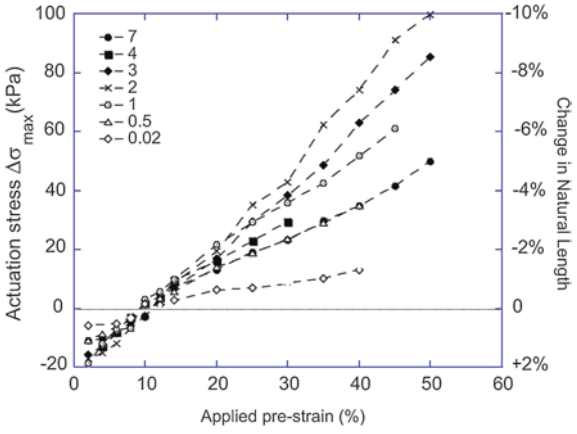

Fig. 2.6 A plot of the maximum change in stress under illumination for different loading so MWNTs in PDMS as a function of applied pre-strain. The *left axis* shows the photoactuation stress and the *right axis* shows the calculated change in length of the sample found from the stress change and the Young's modulus. Reprinted Fig. 2.10 with permission from Ref. [25]. Copyright 2006 by the American Physical Society

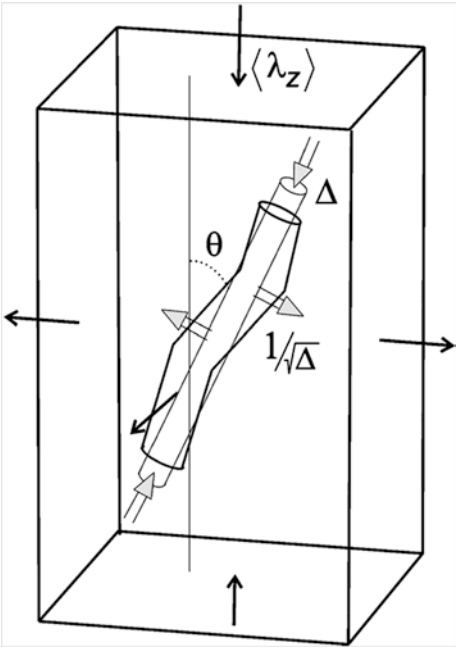

Fig. 2.7 Model of a carbon nanotube in the host matrix and the physical parameters used in the model: Δ, the linear contraction from the photoactuation, and λ_z, the local strain projected on the macroscopic axis. Reprinted Fig. 2.13 with permission from Ref. [25]. Copyright 2006 by the American Physical Society

The photoinduced length change is large, reaching values as high as 10 %. Control experiments using no nanotubes or substituting carbon black for the nanotubes showed no photoactuation. This demonstrates that the primary contributor to the effect arises from the properties of the nanotubes.

A model was developed to explain the magnitude of the photoactuation and the effect of the pre-strain. The distribution of the orientations of the MWNTs in the host polymer were described by an orientation parameter that depends upon the amount of pre-strain. A strain factor, $\Delta = R_z(h\nu)/R_z(0)$, is defined where R is the effective length of the nanotube in the host. Based on the experimental observation that the photoactuation is compressive at high loadings, $\Delta < 1$, and Δ should be proportional to the light intensity (although this was not tested experimentally). A strain tensor can be written in terms of Δ, with terms as shown in Fig. 2.7, relative to the average strain, $\langle \lambda_z \rangle$, shown along the macroscopic z axis. After accounting for the orientational averaging, the calculated strain was found to be

$$\langle \lambda_z \rangle \approx \frac{1}{3}\left(\Delta + \frac{2}{\sqrt{\Delta}}\right) - \frac{2}{5}\varepsilon\left(\frac{1}{\sqrt{\Delta}} - \Delta\right)$$

Setting the strain to 0 allows determination of the crossover pre-strain

$$\varepsilon^* \approx \frac{5\left(2 - \sqrt{\Delta} - \Delta\right)}{6\left(1 + \sqrt{\Delta} + \Delta\right)}$$

At the observed crossover point of ε* ~0.1, Δ is found to be 0.8. Calculation of the length change as a function of pre-strain using the value found for ε* (which is used in the orientational averaging) matched the experimental data well, confirming the essential physics of the model.

2.3.2 Hydrogel Host Materials

A recent paper published by Zhang et al. [27] used poly(N-isopropylacrylamide) (pNIPAM) as the host for SWNTs. In contrast to the rubbers used by the Terentjev group, pNIPAM forms a hydrogel that is thermally responsive. In these hydrogels there is a phase transition between hydrophilic and hydrophobic states that is accompanied by a significant volume change. At lower temperatures pNIPAM is hydrophilic and contains water in the structure. Upon heating to above the transition temperature, ~32–33 °C, the conversion to the hydrophobic state drives the water from the hydrogel, which is responsible for the volume change. Addition of carbon nanotubes allows modification of the hydrogel properties and a chromophore to absorb light.

Samples were prepared by dispersing SWNT, various concentrations up to 1 mg/mL, into water using sodium deoxycholate (chosen to be compatible with pNIPAM) as a surfactant. These were ultrasonicated for an hour, which lead to SWNTs primarily with open ends. The SWNT dispersion was mixed with pNIPAM monomer and polymerized with UV light. For the photoactuation experiments, stripes were laid out that were ~35 μm wide and were illuminated by a laser with a ~20 μm spot size (785 nm, ~30 mW). Exposure to the light caused the pNIPAM to undergo its phase transition, as observed by the sample changing from optically transparent to optically dense and opaque. Although the light was focused on a single stripe, after ~8 s the composite had equilibrated to a black spot of ~150 μm. The process was reversible and fast: after turning the laser off the original state was recovered in ~0.3 s.

The authors attributed the observed effect solely to heating. The SWNT absorb the light and the heat generated by the radiationless decay is transferred to the surrounding medium. Once the phase transition temperature has been attained, the dense, hydrophobic state forms and is accompanied by the volume change. No control experiments were reported to confirm this hypothesis, such as mixing the hydrogel with graphite to see if the same temporal and photoactuation response would have been observed.

2.4 Carbon Nanotube Layered Composites

2.4.1 Carbon Nanotube/Acrylic Elastomer/Poly (vinylchloride) Trilayer Composites

Lu and Panchapakesan [28] developed photoactuators based on bilayers of SWNTs deposited onto polymers. The polymer base was on poly (vinylchloride) (PVC) coated with an acrylic elastomer, i.e. an adhesive tape. SWNTs were dispersed in

isopropyl alcohol at a concentration of 0.16 mg/mL. This suspension was filtered through a poly (tetrafluoroethylene) filter and then rinsed and dried. The SWNT sheet could then be peeled off of the filter to give a free-standing film with a thickness of 30–40 μm. The SWNT film was then directly attached to the acrylic elastomer side of the polymer film. The dimensions of the sample were 30 mm long × 2 mm wide × ~110–120 μm thick. The layers were composed of 50 μm PVC, 30 μm elastomer, and 30–40 μm SWNTs.

To measure the photoactuation, one end of the sample was fixed to a base and the amount of bending determined upon exposure to light. The light source was a halogen lamp and for typical experiments was operated at an intensity of 60 mW/cm^2. The light was illuminated onto the SWNT layer and the bending occurred towards the PVC layer, away from the SWNT layer. The bending was reversible and repeatable for multiple cycles. To measure the strain generated by the photoactuation, the cantilever was clamped on both ends and the strain measured with exposure to light. In all cases the strain was positive, indicating that the sample experienced tension. Rise times of the strain or maximum bending was ~20 s and the return to rest conditions with the light off was about the same.

The strain was measured as a function of light intensity using the white light source and it was found that as the light intensity increased the strain increased linearly to about 40 mW/cm^2 and then nonlinearly at higher light intensities. At the maximum power used, 120 mW/cm^2, the strain reached ~0.3 %. The effect of water on the photoactuation was also measured at 80 mW/cm^2: in a dry environment the strain was found to be ~0.25 % but in water this value was reduced significantly to about ~0.06 %. Finally, using a series of semiconductor lasers, the strain was measured as a function of wavelength (635–1550 nm) at constant, low, power (15 mW/cm^2). While all wavelengths induced photoactuation, the magnitude increased considerably at higher photon energies. At 0.8 eV the strain was ~0.02 %, which was nearly constant up 1.3 eV but then rose to ~0.04 % at 1.9 eV. No comparison to the absorption spectrum of the SWNTs used in the experiment was given but the wavelength response of the photoactuator strain did not appear to follow a typical SWNT spectrum.

The photoactuation was attributed primarily to thermal effects amplified by coupling to the elastomer layer. The absorption of light was thought to heat the sample and introduce electrostatic repulsion in the SWNT bundles. The electrostatic contribution was supported by measuring the photocurrent in the samples. No temperatures change during the photoactuation experiments was reported, so the relative importance of the electrostatic and thermal effects was not determined. The reduction in the measured strain in the aqueous environment could, in part be, explained by heat dissipation into the surrounding environment but some of the reduction is also due to absorption of NIR light by water.

2.4.2 Carbon Nanotube/Photoresist Bilayer Composites

In a follow-up to their initial report, Lu and Panchapakesan [29] developed a photolithography protocol that could be used to make arrays of photoactuator cantilevers.

SWNTs were dispersed in isopropyl alcohol, ~0.1 mg/mL, using ultrasonication but no surfactant. The dispersion was vacuum filtered through a filter composed of a mixed cellulose ester. The thickness of the SWNT layer, ranging from ~40 to ~780 nm, could be controlled by varying the concentration of the nanotubes in the dispersion. The filter membrane containing the nanotube layer was transferred onto a silicon substrate and the cellulose ester dissolved with acetone, leaving a layer of SWNTs with controlled thickness. Photoresist was added to the top of the SWNT layer and standard photolithography was used to form patterns. O_2 etching was used to removed nanotubes in exposed areas and XeF_2 etching was used to remove Si beneath the nanotube layer. For photoactuation experiments, the photoresist (SU8) was not removed. Typical cantilevers were ~300 μm long × 30 μm wide × 7 μm thick—the thickness includes both the SWNT layer and the photoresist.

Photoactuation measurements were done with 808 nm laser light using various powers. The laser was focused an area of ~0.5 × 2 mm^2, indicating that the entire cantilever surface was illuminated. When the cantilever was exposed to light, bending towards the SWNT layer was observed and the tip displacement was linear with respect to laser intensity, as shown in Fig. 2.8. The maximum displacement of the cantilever was ~23 μm under 170 mW of laser power. As in their earlier work, the photoactuation response was attributed to a combination of electrostatic, optical, and thermal effects.

It is interesting to compare the different cantilevers used by Lu and Panchapakesan. In both studies the nanotube layer was primarily composed of SWNTs, although of significantly different thicknesses. In the earlier report the polymer portion was a bilayer—PVC and an acrylic elastomer while in the latter report the polymer was photoresist. The resulting photoactuation is similar in either case but with at least one distinguishable contrast: the observed strain response is nonlinear in the PVC case at laser powers above ~40 mW/cm^2 while when the substrate is photoresist the strain is linear to at least 170 mW/cm^2. No explanation for this has been given.

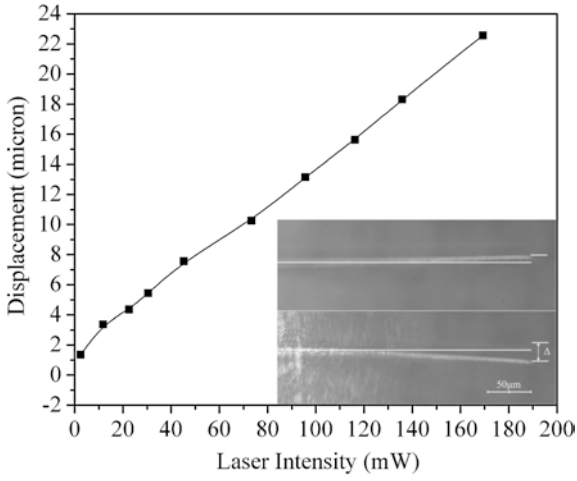

Fig. 2.8 Displacement of a photoresist/SWNT cantilever as a function of laser (808 nm) intensity. The *line* is drawn as a guide for the eye. The inset shows a cross-section of the cantilever under illumination. Reprinted with permission from Ref. [29]. Copyright 2006, American Institute of Physics

2.4.3 Carbon Nanotube/Silicon Nitride Bilayer Composites

More recently, Flannigan and Zewail [30] used 4D electron microscopy to examine the photoactuation of multiwalled carbon nanotubes deposited onto an amorphous silicon nitride grid as the substrate. The MWNTs were deposited onto the Si_3N_4 from an aqueous dispersion made by sonicating the MWNTs with sodium dodecyl sulfate (SDS), followed by centrifiguation. After deposition, the sample was dried at 80 °C under flowing argon for 30 min, cooled, washed with water, and then dried again for 1 h. The amount of residual SDS, if any, was not reported.

Upon exposure to light (776 nm) via a train of femtosecond pulses onto a dense mat of MWNTs, the absorption of light by the MWNTs induced thermal crystallization of the silicon nitride substrate. The crystallization was observed as the sudden appearance of Bragg diffraction spots by the concurrent electron beam. In the absence of light no crystallization was observed, demonstrating that the electron beam was not responsible for the phase change. This implied that the laser pulses were heating the MWNTs to temperatures on the order of 1000 °C and that there is strong coupling between the MWNT mat and the Si_3N_4 substrate. The researchers took advantage of this strong coupling to observe the photoactuation of the MWNTs: the diffraction pattern of the underlying α-Si_3N_4 was used to monitor the photoactuation of the adjacent nanotube network. To monitor the photoactuation, single laser pulses (120 fs) with a low fluence, 6.4 $\mu J/cm^2$ were used. Under these conditions, a radial expansion of each concentric tubule of the MWNTs of 8 ± 0.3 pm was observed, which corresponds to an expansion of the entire nanotube of about 400 pm. No expansion or contraction along the length of the nanotubes were observed.

Based on the temporal response of the photoactuation and the low laser fluence, the authors considered a thermal mechanism unlikely. Using estimates of the absorption coefficient (6×10^4 cm^{-1}), the specific heat capacity (2 J/g•K), and the density (2 g/cm^3), the temperature rise could be no more than 1 °C in the MWNTs. Further, since the time constant of the experiments was found to be 120 ps, only an electronic process was thought to be reasonable to account for the observations. Charge separated polarons were suggested to be formed that could induce an electrostatic repulsion, that was responsible for the mechanical motion. Given the nonuniform nature of the MWNT layer, gradient absorption of the light could also contribute to the photoactuation.

2.4.4 Carbon Nanotube/Nafion Bilayer Composites

Levitsky and Euler [31–33] used SWNTs deposited onto a Nafion substrate to form photoactuating cantilevers. Nafion has a number of interesting properties that led to its choice as a substrate. Nafion contains sulfonic acid group that is effective for hydrogen bonding so Nafion films are always hydrated. This leads

to a pore structure with channels of a few nm that allows water transport through the material. SWNTs were dispersed in chloroform (~0.8–1 mg/mL) by sonication and then air-brushed onto a warm (50 °C) Nafion film (50 μm thick). By repeatedly applying the SWNT suspension with the airbrush, the thickness of the nanotube layer could be controlled. Typical thicknesses for the SWNT layer were 10–20 μm. In the photoactuation experiments, the cantilevers used were 13 mm long × 1 mm wide × 60–70 μm thick. The light source used was a tungsten halogen lamp, a broad band source, with average intensity of 75 mW/cm^2.

When exposed to light the Nafion/SWNT cantilevers exhibited bending that was always has a net response in the direction of the Nafion layer, independent of the direction of the light source. After the light is turned off the cantilever returns to its initial position, demonstrating the reversibility of the system. Two control experiments were done. When SWNTs are airbrushed onto a polyethylene substrate, no photoactuation is observed. Also, when graphite was applied to Nafion, using the same protocols, there again was no photoactuation. These observations suggest that in this system, both the substrate Nafion and the SWNTs play a role in the photoactuation.

Figure 2.9 shows the tip displacement of a cantilever exposed to light as a function of time. When the light is turned on, the initial response is a small bend in the direction of the nanotube layer but quickly (less than a few seconds) reverses to bend towards the Nafion layer. The equilibrium displacement is reached in ~100 s. When the light is turned off, the reverse process takes place: the initial displacement is increased bending towards the Nafion layer for a few seconds and then reverses to relax to the original position in ~100 s. The fast process was only observed under low humidity conditions. At higher humidity levels, only a single exponential rise and decay were observed when the light was turned on and off, respectively.

The photoactuation response is linear with light intensity at low powers, as demonstrated in Fig. 2.10. The slopes of the lines in Fig. 2.10 are similar, suggesting that conversion from light energy to mechanical energy is similar across the

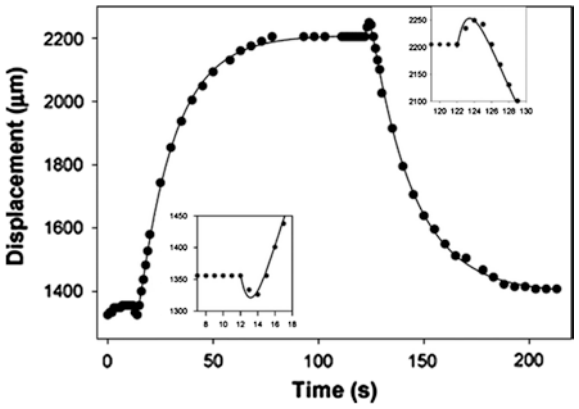

Fig. 2.9 Tip displacement of a Nafion/SWNT cantilever upon exposure to white light as a function of time. The *solid lines* are fits to exponential functions. The *insets* show the first few seconds after the light is turned on (*lower left*) and the light is turned off (*upper right*). Reprinted with permission from Ref. [33]. Copyright 2010 American Chemical Society

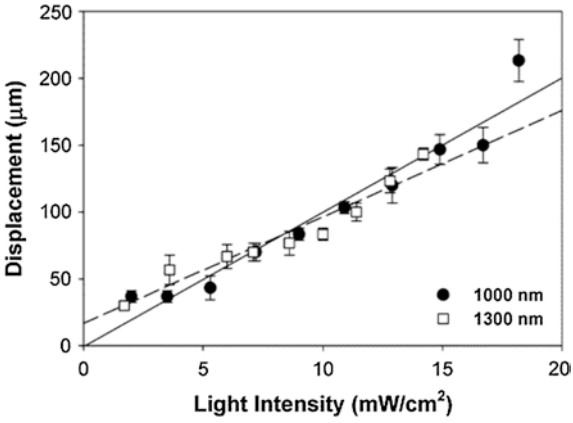

Fig. 2.10 Observed tip displacement of a Nafion/SWNT cantilever as a function of light intensity at 1000 nm (*filled circles*) and 1300 nm (*open squares*). Reprinted with permission from Ref. [32]. Copyright 2006 American Chemical Society

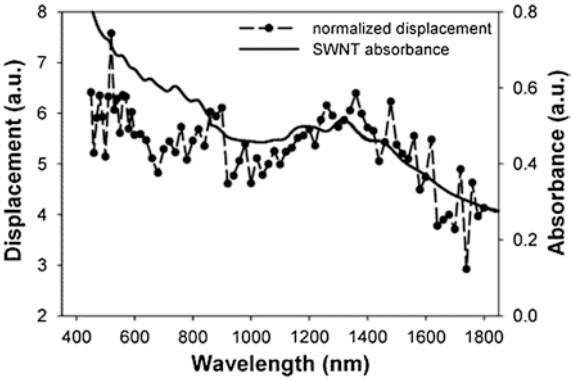

Fig. 2.11 The tip displacement of a Nafion/SWNT cantilever normalized to light intensity as a function of wavelength. For comparison purposes, the solid line shows the absorption spectrum of the SWNTs in the same wavelength region. Reprinted with permission from Ref. [32]. Copyright 2006 American Chemical Society

spectrum. Nafion is transparent in the visible and NIR regions, implying that the light absorption is solely due to the SWNTs. This was confirmed by measuring the photoactuation as a function of wavelength, as shown in Fig. 2.11. The photoactuation spectrum was normalized to a constant light intensity and compared with the absorption spectrum of the SWNTs. The two spectra match well. This implies that even with a mixture of chiralities in the SWNTs, each type of nanotube invokes a similar photoactuation response.

To investigate the role of the Nafion, absorption measurements in the IR region were taken to observe changes in the Nafion structure during photoactuation. Upon exposure to light, with the cantilever anchored to prevent mechanical motion, the intensity of the 2889 nm (3461 cm^{-1}) peak decreased. When the light was turned off, the intensity of this peak returned. This peak arises from the OH stretching of hydrogen-bonded water molecules, which indicates that the internal structure of the Nafion changed during the photoactuation process.

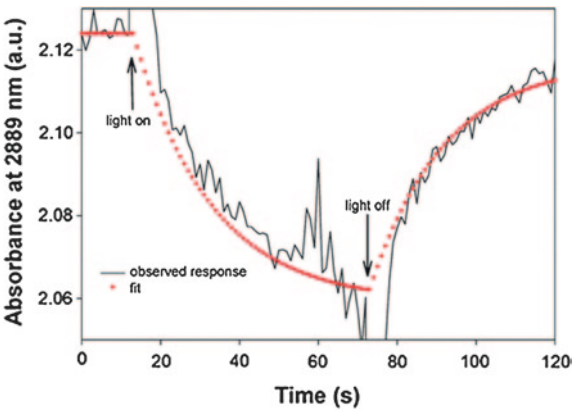

Fig. 2.12 Absorption at 2889 nm (3461 cm^{-1}) of a Nafion/SWNT cantilever as a function of time with light on and light off. The wavelength was chosen to monitor the OH stretching frequency of water trapped in the Nafion pores. The cantilever was anchored to prevent movement. Reprinted with permission from Ref. [33]. Copyright 2010 American Chemical Society

Rate constants for the light-on and light-off processes were determined as a function of the thickness of the SWNT layer. Simple exponential functions were used to model the temporal response:

$$z_{on} = z_{\infty}\left(1 - e^{-k_{on}t}\right)$$

$$z_{off} = z_{\infty}e^{-k_{off}t}$$

where z_{on} and z_{off} are the cantilever tip displacement under light-on and light-off conditions, respectively, z_{∞} is the equilibrium position of the tip displacement with the light on, and k_{on} and k_{off} are the light-on and light-off rate constants, respectively. (A second exponential term was used to model the fast response, but not enough data could be collected to obtain reliable fitting parameters.) Each parameter depends upon the SWNT thickness. The equilibrium displacement, z_{∞}, increases with increasing SWNT thickness, consistent with more light being absorbed driving more photoactuation, but are the same for a given on–off cycle, indicating the reversibility of the photoactuation process. The rate constants k_{on} and k_{off} also vary with the thickness of the SWNT layer, but are not the same. The light-on process has an increasing rate constant as a function of nanotube thickness, indicating that amount of light absorbed influences both the total displacement and the rate of bending. In contrast, the dark relaxation has a decreasing rate constant as function of increasing SWNT thickness. This effect arises because of the mechanical stiffness of the cantilever. As the nanotube thickness increases the modulus of the bilayer composite also increases, which reduces the rate of the recovery to the dark equilibrium state.

The rate constants for the absorption change of the OH stretch used monitor the Nafion were also determined using the same exponential equations. Remarkably, k_{on} and k_{off} were found to match the photoactuation rate constants. This implied that the reorganization of the water molecules trapped in the Nafion pores contributed to the rate limiting process.

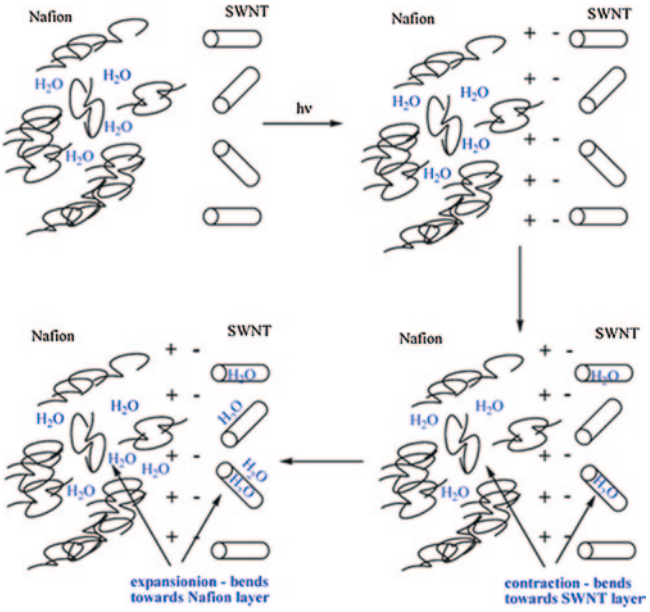

Fig. 2.13 Model used to explain the mechanism of photoactuation in the Nafion/SWNT photoactuation. Reprinted with permission from Ref. [33]. Copyright 2010 American Chemical Society

The effect of a load added to the cantilevers was also measured. As the load increased, the maximum tip displacement decreased. For cantilever with a mass of 1.3 mg, a measurable displacement was found up to a load of ~100 mg, i.e. the photoactuator was able to generate enough force to move more than 75 times its own mass. The rate constants for both light-on and light-off were unchanged as a function of the added mass (Fig. 2.12).

To account for the observations, a model that involved polarization of the Nafion/SWNT interface was described and is shown in Fig. 2.13. The proposed mechanism envisions that charge separates in the SWNT excited state, in part due to the interfacial electric field. The surface charge on the SWNTs became negative and the bulk charge positive, which amplifies the interfacial field. Then, at the interface, water entrapped in the Nafion pores migrates towards the SWNT/Nafion boundary. This induces swelling of the Nafion at the interface and depletion of water in the bulk of the Nafion, causing the cantilever to bend towards the Nafion layer. The proposed mechanism accounts for the major response, but does not account for the short time photoactuation in the reverse direction. It was suggested that the dimensional changes that occur in the SWNTs as a result of the excitation and initial charge separation was responsible for the fast effect.

The proposed model is consistent with the observations of the direction of bending and the influence of humidity on the rate constants. The observation of

simple exponential functions to describe the temporal response requires that the diffusion component of the model occur in a thin film region, a few tens of nanometers from the interface.

2.5 Conclusions

Both single walled and multiwalled carbon nanotubes can be used to prepare materials capable of substantial, macroscopic photoactuation. Amplification of the optomechanical response occurs in composite materials and appears to be an interfacial effect in nearly all cases. In all systems the carbon nanotubes absorb the incident light and then transform the energy into mechanical motion. Generally, it is thought that electrostatic effects dominate the mechanism of photoactuation but the details vary with the structure of the system. Many questions about the nature of photoactuation are still unanswered and there is no unifying understanding, yet.

When small bundles of pure carbon nanotubes are exposed to light there is sufficient charge separation between different individual nanotubes to induce electrostatic repulsion between fibers, which provides enough repulsion to cause deformations on the micron scale. When the bundles are assembled into freestanding films, the photoactuation is amplified to a macroscopic length scale, on the order of millimeters.

When carbon nanotubes are dispersed in a host matrix, the absorption of light by the nanotubes also causes macroscopic deformations. Whether the host is a rubbery polymer or a hydrogel, the energy absorbed by the carbon nanotubes causes a structural change in the surrounding medium. For rubbery polymers, the volume change of the individual carbon nanotubes induces a local strain in the host material, which is amplified throughout the bulk. In the case of hydrogels, the excited state energy of the carbon nanotubes induces a phase change from a hydrophilic to hydrophobic state. Since the hydrophobic state has a higher density, a significant volume change ensues.

Layered composites also lead to macroscopically detectable photoactuation. The best characterized layered systems use polymers as the substrate for the carbon nanotube layer, but the types of polymer vary considerably, including acrylic elastomers, photoresist, and Nafion. In each case the experimental evidence suggests that the interface between the carbon nanotube layer and the substrate layer plays an important role in the optomechanical response. The electrostatic interaction between nanotubes and the substrate is generally attributed as the key feature.

References

1. Baughman, R.H., Cui, C., Zakhidov, A.A., Iqbal, Z., Barisci, J.N., Spinks, G.M., Wallace, G.G., Mazzoldi, A., DeRossi, D., Rinzler, A.G., Jaschinski, O., Roth, S., Kertesz, M.: Carbon nanotube actuators. Science **284**, 1340–1344 (1999)

2. Minett, A., Fràyasse, J., Gang, G., Kim, G.-T., Roth, S.: Nanotube actuators for nanomechanics. Curr. Appl. Phys. **2**, 61–64 (2002)
3. Gartstein, Yu.N, Zakhidov, A.A., Baughman, R.H.: Charge-induced anisotropic distortions of semiconducting and metallic carbon nanotubes. Phys. Rev. Lett. **89**, 045503/1–045503/4 (2002)
4. Sun, G., Kürti, J., Kertesz, M., Baughman, R.H.: Dimensional changes as a function of charge injection in single-walled carbon nanotubes. J. Am. Chem. Soc. **124**, 15076–15080 (2002)
5. Landi, B.J., Raffaelle, R.P., Heben, M.J., Alleman, J.L., VanDerveer, W., Gennett, T.: Single wall carbon nanotube–nafion composite actuators. Nano Lett. **2**, 1329–1332 (2002)
6. Tahhan, M., Truong, V.-T., Spinks, G.M., Wallace, G.G.: Carbon nanotube and polyaniline composite actuators. Smart Mater. Struct. **12**, 626–632 (2003)
7. Levitsky, I.A., Kanelos, P.T., Euler, W.B.: Novel actuating system based on a composite of single-walled carbon nanotubes and an ionomeric polymer. Mater. Res. Soc. Symp. Proc. **785**, D9.1.1–D9.1.6 (2004)
8. Levitsky, I.A., Kanelos, P., Euler, W.B.: Electromechanical actuation of composite material from carbon nanotubes and ionomeric polymer. J. Chem. Phys. **121**, 1058–1065 (2004)
9. Minett, A., Fràysse, J., Gang, G., Kim, G.-T., Roth, S.: Nanotube actuators for nanomechanics. Curr. Appl. Phys. **2**, 61–64 (2002)
10. Gartstein, Yu.N, Zakhidov, A.A., Baughman, R.H.: Charge-induced anisotropic distortions of semiconducting and metallic carbon nanotubes. Phys. Rev. Lett. **89**, 045503/1–045503/4 (2002)
11. Liu, J.Z., Zheng, Q., Jiang, Q.: Effect of bending instabilities on the measurements of mechanical properties of multiwalled carbon nanotubes. Phys. Rev. B. **67**, 075414/1–075414/8 (2003)
12. Li, C., Chou, T.-W.: Single-walled carbon nanotubes as ultrahigh frequency nanomechanical resonators. Phys. Rev. B **68**, 073405/1–073405/3 (2003)
13. Bozovic, D., Bockrath, M., Hafner, J.H., Lieber, C.M., Park, H., Tinkham, M.: Plastic deformations in mechanically strained single-walled carbon nanotubes. Phys. Rev. B **67**, 033407/1–033407/4 (2003)
14. Verissimo-Alves, M., Koiller, B., Chacham, H., Capaz, R.B.: Electromechanical effects in carbon nanotubes: *ab initio* and analytical tight-binding calculations. Phys. Rev. B **67**, 161401/1–161401/4 (2003)
15. Cao, J., Wang, Q., Dai, H.: Electromechanical properties of metallic, quasimetallic, and semiconducting carbon nanotubes under stretching. Phys. Rev. Lett. **90**, 157601/1–157601/4 (2003)
16. Farajian, A.A., Yakobson, B.I., Mizuseki, H., Kawazoe, Y.: Electronic transport through bent carbon nanotubes: nanoelectromechanical sensors and switches. Phys. Rev. B **67**, 205423/1–205423/6 (2003)
17. Sapmaz, S., Blanter, Ya.M., Gurevich, L., van der Zant, H.S.J.: Carbon nanotubes as nanoelectromechanical systems. Phys. Rev. B. **67**, 235414/1–235414/7 (2003)
18. Minot, E.D., Yaish, Y., Sazonova, V., Park, J.-Y., Brink, M., McEuen, P.L.: Tuning carbon nanotube band gaps with strain. Phys. Rev. Lett. **90**, 156401/1–156401/4 (2003)
19. Pastewka, L., Kosinen, P., Elsasser, C., Moseler, M.: Understanding the microscopic processes that govern the charge-induced deformation of carbone nanotubes. Phys. Rev. B Cond. Matt. Phys. **180**, 155428/1–155428/16 (2009)
20. Zhang, Y., Iijima, S.: Elastic response of carbon nanotube bundles to visible light. Phys. Rev. Lett. **82**, 3472–3475 (1999)
21. Cronin, S.B., Yin, Y., Walsh, A., Capaz, R.B., Stolyrov, A., Tangney, P., Cohern, M.L., Louie, S.G., Swan, A.K., Ünlü, M.S., Goldberg, B.B., Tinkham, M.: Temperature dependence of the optical transition energies of carbon nanotubes: the role of electron-phonon coupling and thermal expansion. Phys. Rev. Lett. **96**, 127403/1–127402/4 (2006)
22. Ahir, S.V., Terentjev, E.M., Lu, S.X., Panchapakesan, B.: Thermal fluctuations, stress relaxation, and actuation in carbon nanotube networks. Phys. Rev. B Cond. Matt. Phys. **76**, 165437/1–165437/6 (2007)
23. Ahir, S.V., Terentjev, E.M.: Photomechanical actuation in polymer-nanotube composites. Nat. Mater. **4**, 491–495 (2005)

24. Ahir, S.V., Terentjev, E.M.: Fast relaxation of carbon nanotubes in polymer composite actuators. Phys. Rev. Lett. **96**, 133902/1–133902/4 (2006)
25. Ahir, S.V., Squire, A.M., Tajbakhsh, A.R., Terentjev, E.M.: Infrared actuation in aligned polymer-nanotube composites. Phys. Rev. B Cond. Matt. Phys. **73**, 085420/1–0854201/2 (2006)
26. Ahir, S., Huang, Y.Y., Terentjev, E.M.: Polymers with aligned carbon nanotubes: active composite materials. Polymer **49**, 3841–3854 (2008)
27. Zhang, X., Pint, C.L., Lee, M.H., Schubert, B.E., Jamshidi, A., Takei, K., Ko, H., Gillies, A., Bardhan, R., Urban, J.J., Wu, M., Fearing, R., Javey, A.: Optically- and thermally-responsive programmable materials based on carbon nanotube-hydrogel polymer composites. NanoLetters **11**, 3239–3244 (2011)
28. Lu, S.X., Panchapakesan, B.: Optically driven nanotube actuators. Nanotechnology **16**, 2548–2554 (2005)
29. Lu, S.X., Panchapakesan, B.: Nanotube micro-optomechanical actuators. Appl. Phys. Lett. **88**, 253107/1–253107/3 (2006)
30. Flannigan, D.J., Zewail, A.H.: Optomechanical and crystallization phenomena visualized with 4D electron microscopy: interfacial carbon nanotubes on silicon nitride. NanoLetters **10**, 1892–1899 (2010)
31. Levitsky, I.A., Kanelos, P.T., Viola, E.A., Euler, W.B.: Photoactuation in nafion-carbon nanotube bilayer composites. Proc. SPIE Nanosens. Mater. Device **II**(6008), 600802/1–600802/6 (2005)
32. Levitsky, I.A., Kanelos, P.T., Woodbury, D.S., Euler, W.B.: Photoactuation from a carbon nanotube–nafion bilayer composite. J. Phys. Chem. B **110**, 9421–9425 (2006)
33. Viola, E.A., Levitsky, I.A., Euler, W.B.: Kinetics of photoactuation in single wall carbon nanotube–nafion bilayer composite. J. Phys. Chem. C **114**, 20258–20266 (2010)

http://www.springer.com/978-1-4471-4825-8

Photophysics of Carbon Nanotubes Interfaced with Organic and Inorganic Materials

Levitsky, I.A.; Euler, W.B.; Karachevtsev, V.A.

2012, VIII, 164 p., Hardcover
ISBN: 978-1-4471-4825-8